Thermal self-action of CW laser radiation propagating vertically in a fluid

A. N. Bogaturov, V. I. Zuev, and V. M. Ol'khov

The Institute of Atmospheric Physics of the Academy of Sciences of the USSR
(Submitted 12 May 1987)
Zh. Eksp. Teor. Fiz. **94**, 152–165 (August 1988)

Thermal self-defocusing of laser radiation is investigated in conditions of induced photoabsorption convection (PC) together with the characteristic thermal self-action length and the velocity and temperature of convective flow. The dependence of these quantities on fluid and beam parameters is determined by dimensional analysis in well developed photoabsorption convection. The expressions obtained in the present study are in good agreement with experimental results in moderate PC conditions.

1. INTRODUCTION

One of the principal effects from the propagation of powerful radiation in a medium is heating of the medium by photoabsorption. The development of temperature gradients in fluids and gases results in convective flows that can significantly influence heat transport in the medium and therefore the propagation of the light beam.[1] There are many studies devoted to investigating the self-action of light beams in the presence of natural or induced convective flows for the case of horizontal radiation propagation.[1–3] In this case motion of the medium is transverse to the optical beam axis so that both the temperature distribution and the refractive index are determined by the transverse beam shape. In the case of vertical radiation propagation in an initially quiescent medium heat transport runs largely along the light beam axis. In other words self-action is nonlocal along the longitudinal coordinate of the light beam, which causes changes in the parameters characterizing the radiation propagation process compared to the case of a horizontal beam or self-action in a static medium.

A theoretical analysis and experimental investigation of thermal self-action of radiation for the case of vertical propagation in conditions of photoabsorption convection (PC) have not been carried out to date. The present study is aimed at such an investigation of this proces.

The analysis of the fundamental laws of thermal self-action in PC conditions is based on treating the hydrodynamic and geometric optics equations for the case of cylindrical symmetry by means of similarity theory. Two limits are considered: Moderate and well developed convection. The analysis of nonlinear effects in well developed PC yields fundamental scale relations for quantities describing convective flow and for the characteristic thermal self-action length.

Nonlinear effects in moderate PC are observed directly in the experiment and are therefore investigated in greater detail in the theoretical analysis. Therefore an approximate analysis of hydrodynamic equations is used to derive expressions that determine the velocity and temperature of the convective flow. This made it possible to achieve closure of the geometrical optics equations and to analyze these equations qualitatively.

Radiation was directed upward for the experimental investigations. The PC velocities and the temperature of the medium were measured together with the divergence of the light beams exiting the fluid. The radiation beam power, layer thickness and type of fluid were varied in the experiment. The experimental data from the entire series of measurements were in agreement with theoretical results for moderate PC conditions. The present study has therefore obtained experimental confirmation of the existence of moderate PC in fluids.

2. FORMULATION OF THE PROBLEM

It is difficult to solve the hydrodynamic and geometrical optics equations self-consistently even by using modern computer technology. To date a numerical investigation of hydrodynamic equations for the case of vertical propagation of heating radiation has been carried out only in the case of a prescribed light beam.[4] Dimensional analysis has been applied repeatedly in PC investigations for a prescribed horizontal source to obtain fundamental relations; the results have been confirmed in numerical experiments.[4,7,8] We will apply dimensional analysis to the problem of the nonlinear propagation of a vertical optical beam.

The purpose of the present study is to determine the characteristic thermal self-action length L_{NL}. The subsequent analysis involves determining the influence of nonlinear beam distortion on the scale factors of convective motion.

We will assume that the fluid layer is heated by a vertical axisymmetrical light beam. We will consider the case most characteristic of practical applications: A transverse beam scale r_0 significantly less than all other longitudinal and transverse spatial scales of the problem. In a geometrical optics approximation the light beam propagation is described by the following system of equations by virtue of the symmetry of the problem:

$$\frac{\partial J}{\partial z}+\frac{1}{r}\frac{\partial}{\partial r}(rqJ)+\alpha J=0,$$
$$\frac{\partial q}{\partial z}+q\frac{\partial q}{\partial r}=-\frac{1}{n_0}\left|\frac{dn}{dT}\right|\frac{\partial T}{\partial r}, \qquad (1)$$

where z is the longitudinal coordinate (in the direction of beam propagation), r is the radial coordinate, $J(z,r)$ is the light beam intensity, $q=\partial\varphi/\partial r$, φ is the correction to the eikonal of a plane wave, α is the absorption coefficient, $T(z,r)$ is the change in the temperature of the medium due to photoabsorption heating, and $n=n_0-|dn/dT|T$ is the refractive index of the fluid.

The photoabsorption convective steady state of a viscous thermally-conducting fluid is described by the system

 0038-5646/88/081602-08$04.00

of Navier-Stokes equations in the Boussinesq approximation[4,9,10]:

$$\frac{\partial V}{\partial z}+\frac{1}{r}\frac{\partial}{\partial r}(rU)=0,$$
$$V\frac{\partial T}{\partial z}+U\frac{\partial T}{\partial r}-\chi\Delta T=\frac{\alpha}{\rho_0 c_p}J; \tag{2}$$

$$\nu\Delta V-\left(V\frac{\partial V}{\partial z}+U\frac{\partial V}{\partial r}\right)=mg\beta T+\frac{\partial}{\partial z}\frac{p}{\rho_0},$$
$$\nu\left(\Delta U-\frac{U}{r^2}\right)-\left(V\frac{\partial U}{\partial z}+U\frac{\partial U}{\partial r}\right)=\frac{\partial}{\partial r}\left(\frac{p}{\rho_0}\right), \tag{3}$$

where V and U are the vertical and radial velocity components of the fluid, respectively, ν is the kinematic viscosity, g is the gravitational acceleration, β is the coefficient of thermal expansion, χ is the thermal conductivity coefficient, ρ_0 is the fluid density, c_p is the specific heat at constant pressure, p is the deviation from hydrostatic pressure, $m=1$ for the case of top-to-bottom laser illumination and $m=-1$ in the reverse case, $\Delta=\Delta_\perp+\partial^2/\partial z^2$ is the Laplacian, and

$$\Delta_\perp=\frac{1}{r}\frac{\partial}{\partial r}\left(r\frac{\partial}{\partial r}\right)$$

is the transverse Laplacian.

The function p/ρ_0 can easily be eliminated from (3) and this system can then be written as a single equation

$$\nu\Delta^2 V=\Delta_\perp\left\{mg\beta T+V\frac{\partial V}{\partial z}+U\frac{\partial V}{\partial r}+\frac{\partial}{\partial z}\int_r^\infty\left(V\frac{\partial U}{\partial z}+U\frac{\partial U}{\partial r'}\right)dr'\right\}. \tag{4}$$

The primary PC regularities can be obtained from the relations between the inertial and viscous forces and between heat release and thermal and mass transport. The results of such an analysis[4–6] reveal that three regimes of free conduction are possible in photoabsorption: Weak, moderate and well developed convection. The transition from weak to moderate and from moderate to well developed convection is characterized by an increase in the amplitude of the vertical velocity component of the convective flow. Taking into account the natural boundary condition $V=0$ in the longitudinal coordinate for the vertical velocity component we conclude that only a single convective flow regime (aside from weak convection) is possible along the entire radiation propagation path in the case of vertical beam propagation. In the subsequent sections we will, however, consider the nonlinear behavior of radiation in isolated PC conditions. In this case we will assume that the regions having conditions characterized by the lowest vertical flow velocity component are concentrated in layers that are thin compared to L_{NL} near the illuminated fluid boundary, so that it is possible to ignore their contribution to beam defocusing. An estimate of this contribution will be given in Sec. 5 for the case implemented in the experiment.

In the case of weak convection the heat liberated by photoabsorption is transported away from the beam through thermal conductivity. The nonlinear action of the radiation in this case is therefore identical to the laser beam defocusing in a static medium examined in Ref. 11 and will not be analyzed.

3. MODERATE CONVECTION

Moderate convection conditions occur when the buoyancy is balanced by the viscosity, and heat is transported away from the beam by convection.[6] We will introduce dimensionless variables that will make it possible to identify the primary terms for such conditions in the hydrodynamic equations:

$$J(z,r)=J_0 e^{-\alpha z}I(z.r), \tag{5}$$

where J_0 is the intensity of the beam at the fluid boundary,

$$z=Lx,\quad r=r_0\rho,$$
$$V=V_0 v,\quad U=V_0(r_0/L)u,\quad T=T_0\theta. \tag{6}$$

Here $L=\min\{1/\alpha, H\}$, H is the thickness of the fluid layer, and

$$V_0=\left(\frac{\alpha g\beta}{\nu\rho_0 c_p}J_0 r_0^2 L\right)^{1/2},\quad T_0=\left(\frac{\alpha\nu}{g\beta\rho_0 c_p}\frac{J_0 L}{r_0^2}\right)^{1/2}. \tag{7}$$

In new variables Eqs. (2), (4) will take the following form:

$$\frac{\partial v}{\partial x}+\frac{1}{\rho}\frac{\partial}{\partial\rho}(\rho u)=0, \tag{8}$$

$$v\frac{\partial\theta}{\partial x}+u\frac{\partial\theta}{\partial\rho}-\exp(-\alpha Lx)I=\left\{\Delta_\perp\theta+\frac{1}{\gamma^2}\frac{\partial^2\theta}{\partial x^2}\right\}\Big/\mathrm{Pr}\,Q^{1/2}, \tag{9}$$

$$\left\{\Delta_\perp+\frac{1}{\gamma^2}\frac{\partial^2}{\partial x^2}\right\}^2 v-m\Delta_\perp\theta=Q^{1/2}\Delta_\perp\left\{v\frac{\partial v}{\partial x}+u\frac{\partial v}{\partial\rho}+\frac{1}{\gamma^2}\frac{\partial}{\partial x}\int_\rho^\infty\left(v\frac{\partial u}{\partial x}+u\frac{\partial u}{\partial\rho'}\right)d\rho'\right\}, \tag{10}$$

where $\mathrm{Pr}=\nu/x$ is the Prandtl number, $\gamma=L/r_0\gg 1$, and

$$Q=\frac{\alpha g\beta}{\nu^3\rho_0 c_p}\frac{J_0 r_0^6}{L}. \tag{11}$$

The dimensionless parameter Q characterizing the density of the internal heat sources will be called the thermal complex, consistent with Ref. 6.

This regime is achieved when it is possible to ignore the influence of thermal conductivity and inertial forces in (9), (10) (the corresponding terms are isolated on the right hand sides of the equations). In other words, moderate convection exists when

$$\mathrm{Pr}^{-2}\ll Q\ll 1. \tag{12}$$

In this section we will assume that relations (12) hold and that the right hand sides of (9), (10) vanish. In this case we can express the vertical velocity component from Eq. (10) through the fluid temperature. For example, in the case $0\leqslant x,\rho<\infty$. $L=1/\alpha$, taking into account the boundary condition $v(x,\rho)_{x=0}=0$, we will have $v(x,\rho)=v_{\mathrm{I}}(x,\rho)+v_{\mathrm{II}}(x,\rho)$, where

$$v_I(x,\rho)=m\Big[-\ln\gamma\int_0^\infty d\rho'\,\rho'\theta(x,\rho')+\ln\rho\int_0^\rho d\rho'\,\rho'\theta(x,\rho')$$

$$+\int_\rho^\infty d\rho'\,\rho'\theta(x,\rho')\ln\rho'-\frac{1}{2}\int_0^\pi\frac{d\varphi}{\pi}\int_0^\infty d\rho'\,\rho'\theta(x,\rho')f(x,a)\Big],$$

$$v_{II}(x,\rho)=\frac{m}{4}\int_0^\pi\frac{d\varphi}{\pi}\int_0^\infty d\rho'\,\rho'\Big[\int_x^\infty dt\frac{\partial\theta(t,\rho')}{\partial t}$$

$$\cdot\{f(t-x,a)-f(t+x,a)\}+\int_0^x dt\frac{\partial\theta(t,\rho')}{\partial t}\{2f(x,a)-f(x-t,a)$$

$$-f(x+t,a)\}\Big],$$

$$f(x,a)=2\ln\,[x+(x^2+a^2)^{1/2}]-x/(x^2+a^2)^{1/2},$$
$$a^2=\gamma^{-2}(\rho^2+\rho'^2+2\rho\rho'\cos\varphi). \qquad (13)$$

To analyze these expressions further, we will assume $\gamma\gg 1$. It follows directly from Eq. (9) with the right-hand side set to zero that in the heating beam region with the exception of the layer near the upper boundary where $(\partial/\partial x)v(x,0)<0$ holds the transverse scale of the temperature distribution of the flow coincides with the transverse scale of the beam which, by definition, in the variable ρ is characterized by a value ~ 1. We can therefore set $\alpha=0$ in Eqs. (13) for $x\gg+/\gamma$ and $\rho\ll\gamma$. It is then easy to find that $v_{II}\ll v_I$ for $\rho\ll\gamma$, with the exception of the regions $0\leqslant x\sim 1/\gamma$ and $x\geqslant 1$. It follows from $v_I(x,\rho)$ that in the neighborhood of the optical beam ($\rho\sim 1$) that we have

$$|v(x,0)-v(x,\rho)|\ll v(x,0), \qquad (14)$$

where we have for the vertical velocity component on the flow axis

$$v(x,0)=m\Big\{[-\ln(2\gamma x)+{}^1/_2]\int_0^\infty d\rho'\,\rho'\theta(x,\rho')$$

$$+\int_0^\infty d\rho'\,\rho'\theta(x,\rho')\ln\rho'\Big\}. \qquad (15)$$

We will now determine the dimensionless flow temperature. Taking into account (8) we see clearly that it is possible to integrate equation (9) with respect to $\theta(x,\rho)$ along the flow lines given by the equation

$$\int_0^{\rho(x)} d\rho'\,\rho'v(x,\rho')=\text{const}. \qquad (16)$$

In the general case, assuming that the base on which the fluid layer rests is isothermal ($\theta(x_L,\rho)=0$, where x_L is the coordinate of the lower boundary of the layer), and remembering that in this case the turning points of the flow lines ($(d/dx)\rho(x)=\infty$) lie beyond the thermal source ($\rho(x)\sim\gamma\gg 1$), this integral can be written in the following manner:

$$\theta(x,\rho)=\int_{x_L}^x d\xi\,\frac{\exp(-\alpha L\xi)I(\xi,\rho(\xi))}{v(\xi,\rho(\xi))}. \qquad (17)$$

Recalling (14) we can set $v(x,\rho)=v(x,0)$ in (16), (17). Then we obtain the following expression for the dimensionless flow temperature:

$$\theta(x,\rho)=\int_{x_L}^x d\xi\,\frac{\exp(-\alpha L\xi)I(\xi,\rho[v(x,0)/v(\xi,0)]^{1/2})}{v(\xi,0)}. \qquad (18)$$

Substituting (18) into (15) we can express the axial flow velocity through the beam and fluid parameters. Such an expression is found analogously in other spatial configurations of the fluid layer. We will provide dimensionless expressions for the axial velocity of the flow in two characteristic cases:

a) In the case of a broad fluid layer ($0\leqslant r\leqslant\Lambda$, $\Lambda\gg L\gg r_0$)

$$V(z)=(-m)\Big\{\frac{\alpha g\beta P}{2\pi\nu\rho_0 c_p}(-m)\cdot\int_{z_L}^z dt\exp(-\alpha t)\ln\Big[\frac{2z(H-z)}{r(t)H}\Big]\Big\}^{1/2}, \qquad (19)$$

b) in the case of narrow fluid cloumn ($L\gg\Lambda\gg r_0$)

$$V(z)=(-m)\Big[\frac{\alpha g\beta P}{2\pi\nu\rho_0 c_p}(-m)\int_{z_L}^z dt\,e^{-\alpha t}\ln\Big(\frac{\Lambda}{r(t)}\Big)\Big]^{1/2}. \qquad (20)$$

In the last case we assume the beam is directed along the column axis. In expressions (19), (20), $r(t)$ coincides with the beam radius in the cross section $z=t$ to within a factor of order unity. The flow temperature is determined from (7), (18) in the following manner:

$$T(z,r)=\Big(\frac{2\pi\alpha\nu}{g\beta\rho_0 c_p PL}\Big)^{1/2}J_0(-m)\cdot\int_{z_1}^z dt\,\frac{e^{-\alpha t}I[t,r(\sigma(z)/\sigma(t))^{1/2}]}{\sigma(t)}, \qquad (21)$$

where for case a)

$$\sigma(z)=\Big[\frac{-m}{L}\int_{z_L}^z dt\,e^{-\alpha t}\ln\Big(\frac{2z(H-z)}{r(t)H}\Big)\Big]^{1/2}, \qquad (22)$$

for case b)

$$\sigma(z)=\Big[\frac{-m}{L}\int_{z_L}^z dt\,e^{-\alpha t}\ln\Big(\frac{\Lambda}{r(t)}\Big)\Big]^{1/2}. \qquad (23)$$

Knowing expression (21) for the flow temperature, we can analyze the optical beam propagation process. We will take $r_0\ll L_{NL}\ll L$. We will also go over to dimensionless form in the system (1). For this we use (5) and introduce the variables $t=z/L_{NL}$, $\rho=r/r_0$, $s=qL_{NL}/r_0$. Subject to (21) the system (1) takes the following form:

$$\frac{\partial I}{\partial t}+\frac{1}{\rho}\frac{\partial}{\partial\rho}(\rho sI)=0,$$

$$\frac{\partial s}{\partial t}+s\frac{\partial s}{\partial\rho}=\Big(\frac{L_{NL}}{r_0}\Big)^3\Phi m\int_{t_L}^t d\xi\,\frac{\exp(-\alpha L_{NL}\xi)}{\sigma(L_{NL}\xi)/\sigma_0}\times\frac{\partial}{\partial\rho}I\Big(\xi,\rho\Big[\frac{\sigma(L_{NL}t)}{\sigma(L_{NL}\xi)}\Big]^{1/2}\Big), \qquad (24)$$

where we introduce the convention

$$\Phi=\frac{1}{n_0}\Big|\frac{dn}{dT}\Big|\frac{J_0}{\sigma_0}\Big[\frac{2\pi\alpha\nu r_0^2}{g\beta\rho_0 c_p PL}\Big]^{1/2}, \qquad (25)$$

σ_0 is a typical value of the function $\sigma(L_{NL}t)$ ($\sigma(L_{NL}t)\approx\sigma_0$ for $t\approx 1$). From (24) we find that the thermal self-action length is determined from the relation

$$(L_{NL}/r_0)^3\Phi=1. \tag{26}$$

It follows from (25) that L_{NL} is determined by both the intensity scale (for example, the axial intensity of Gaussian beams), and the beam power. However in the general case these two properties are related. Therefore for simplicity we will henceforth replace J_0 with P/r_0^2 in (25).

Let the fluid be irradiated by the laser from above: $m=1$, $z_L=H$. Then for $L_{NL}\ll L$ we will have from (22), (23) in case a)

$$\sigma_0\approx\left[\frac{1-e^{-\alpha H}}{\alpha L}\ln\left(\frac{L_{NL}}{r_0}\right)\right]^{1/2}, \tag{27a}$$

while in case b)

$$\sigma_0\approx\left[\frac{1-e^{-\alpha H}}{\alpha L}\ln\left(\frac{\Lambda}{r_0}\right)\right]^{1/2}. \tag{27b}$$

Substituting (27) into (26) in case a) we obtain the following equation for determining L_{NL}:

$$\left(\frac{L_{NL}}{r_0}\right)^6\Big/\ln\left(\frac{L_{NL}}{r_0}\right)$$

$$=(1-e^{-\alpha H})g\beta\rho_0c_pr_0^2\left[2\pi\left(\frac{1}{n_0}\left|\frac{dn}{dT}\right|\right)^2\alpha^2\nu P\right]^{-1}=A. \tag{28}$$

Taking into account $L_{NL}\gg r_0$, we can estimate the solution of (28) in the following manner:

$$L_{NL}=\left\{\frac{\ln A}{12\pi}(1-e^{-\alpha H})g\beta\rho_0c_pr_0^8\left[\alpha^2\left(\frac{1}{n_0}\left|\frac{dn}{dT}\right|\right)^2\nu P\right]^{-1}\right\}^{1/6}. \tag{29}$$

For case b) we have directly from (26), (27)

$$L_{NL}=\left\{\frac{\ln(\Lambda/r_0)}{2\pi}(1-e^{-\alpha H})g\beta\rho_0c_pr_0^8\cdot\left[\alpha^2\left(\frac{1}{n_0}\left|\frac{dn}{dT}\right|\right)^2\nu P\right]^{-1}\right\}^{1/6}. \tag{30}$$

If we now represent the functions $I(t,\rho)$ and $s(t,\rho)$ as

$$I(t,\rho)=\frac{1}{R^2(t)}\sum_{n=0}^{\infty}I_n(t)\left(-\frac{\rho^2}{R^2(t)}\right)^n,\quad I_0(t)=I_0(0),$$

$$s(t,\rho)=\frac{\rho}{R(t)}\left\{\frac{dR}{dt}+\sum_{n=1}^{\infty}\frac{\beta_n(t)}{R(t)}\left(-\frac{\rho^2}{R^2(t)}\right)^n\right\}, \tag{31}$$

then (24) can be written as a system of equations for R, I_n, β_n. It follows from this system that for $1\lesssim t\to\infty$

$$dR/dt\approx\text{const},\quad R(t)\approx t\cdot\text{const},\quad \beta_n(t)\sim\ln t,\quad I_n(t)\approx I_n(\infty).$$

Therefore direct beam self-action and distortion to the initial beam shape occur in the range $0\leqslant t\sim 1$ ($0\leqslant z-L_{NL}$). Nonlinear effects are virtually absent outside this range and the wavefront (accurate to terms $\sim t^{-1}\ln t$) is spherical, the beam shape is not distorted and the only change is in its transverse dimensions $r(z)\approx\text{const}\,(r_0/L_{NL})z$ where the beam divergence $\psi\approx\text{const}\,(r_0/L_{NL})$, with proportionality factors ~ 1. These relations were confirmed in experimental studies (see Sec. 5).

Now assume the light beam is propagating upward: $m=-1$, $z_L=0$. Then taking into account $\alpha L_{NL}\ll 1$, we will have from (22), (23) in case a)

$$\sigma_0\approx\left[\frac{L_{NL}}{L}\ln\left(\frac{L_{NL}}{r_0}\right)\right]^{1/2}, \tag{32a}$$

in case b)

$$\sigma_0\approx\left[\frac{L_{NL}}{L}\ln\left(\frac{\Lambda}{r_0}\right)\right]^{1/2}. \tag{32b}$$

Analogous to expressions (29), (30) we obtain from (32), (25) in case a)

$$L_{NL}=\left\{\frac{\ln B}{10\pi}g\beta\rho_0c_pr_0^8\left[\alpha\nu\left(\frac{1}{n_0}\left|\frac{dn}{dT}\right|\right)^2P\right]^{-1}\right\}^{1/5},$$

$$B=g\beta\rho_0c_pr_0^3\left[\alpha\nu\left(\frac{1}{n_0}\left|\frac{dn}{dT}\right|\right)^2P\right]^{-1}, \tag{33a}$$

and in case b)

$$L_{NL}=\left\{\frac{\ln(\Lambda/r_0)}{2\pi}g\beta\rho_0c_pr_0^8\left[\alpha\nu\left(\frac{1}{n_0}\left|\frac{dn}{dT}\right|\right)^2P\right]^{-1}\right\}^{1/5}. \tag{33b}$$

We will examine the influence of thermal beam expansion on the scale quantities characterizing convective flow. It follows directly from (19), (20) that the influence of this effect on the axial flow velocity is manifested as a logarithmic dependence on the beam radius and therefore the scale dependence of the velocity on the light beam parameters remains the same as in the case of a prescribed thermal source: $V\sim P^{1}\gtrsim^{2}$. From (21) and the representation (31) we can obtain the following expression for the axial temperature of the flow:

$$T(z,0)=C\tilde{T}\frac{(-m)}{L}\int_{z_L}^{z}dt\frac{e^{-\alpha t}}{\sigma(t)R^2(t)},\quad \tilde{T}=\left(\frac{2\pi\alpha\nu PL}{g\beta\rho_0c_pr_0^4}\right)^{1/2}, \tag{34}$$

where $C=J(0,0)r_0^2/P$ and $\tilde{T}$ is the characteristic temperature value in the case of zero heating beam expansion. For the case of upward propagation and $L_{NL}\ll L$ taking into account that $R(z)\sim z/L_{NL}$ we will have the following expression for the temperature scale of the convective flow in the range $0\leqslant z\sim L_{NL}$

$$T\sim\frac{L_{NL}}{L}\tilde{T}\sim\left(\frac{P}{r_0^2}\right)^{1/6}, \tag{35}$$

while for $z\gg L_{NL}$

$$T\sim(L_{NL}/L)^2\tilde{T}\sim(Pr_0^4)^{1/6}. \tag{36}$$

The dependence on beam parameters is identified explicitly on the right hand side in relations (35), (36). For the case of downward beam propagation we find similarly that the temperature scale for $L_{NL}\ll L$ is determined by substituting L with L_{NL} (33) in the expression for $\tilde{T}$:

$$T \sim \left\{ \alpha \nu P \left[\left(\frac{1}{n_0} \left| \frac{dn}{dT} \right| \right)^{1/2} g \beta \rho_0 c_p r_0^3 \right]^{-1} \right\}^{2/5}. \quad (37)$$

Expressions (35), (36) describe the following effect: Strong radiation self-action reduces the absolute temperature values of convective flow and causes a vertical temperature gradient approaching the upper surface compared to the case in which the light beam is prescribed. In the case of upward propagation both the absolute temperature and the vertical gradient drop.

In concluding this section we wish to make the following comment. An approximate expression was derived in this analysis for the flow temperature (18). Using this expression it is possible to evaluate the influence of the right sides of Eqs. (9), (10) on the derived solutions by means of perturbation theory. For example for case b) implemented in the experiment this analysis implies that it is possible to ignore the influence of thermal conductivity and inertial forces on the axial flow velocity for

$$\mathrm{Pr}^{-2} \ll Q' < 200 (r_0/\Lambda)^4 \ln^3 (\Lambda/r_0), \quad (38)$$

where

$$Q' = P r_0^4 \alpha g \beta / 2\pi L \nu^3 \rho_0 c_p.$$

The parameter Q' is the thermal complex (11), where we use the value $P/2r_0^2$ obtained from examining the beam intensity scale J_0.

4. DEVELOPED CONVECTION

Well developed convection differs from moderate PC in that the buoyancy forces do not balance the viscous forces but rather the inertial forces. In order to directly reflect this difference in the hydrodynamic equations we will introduce new dimensionless variables. We will use relations (5), (6) for this purpose, although in this section we will assume that

$$V_0 = \left[\frac{J_0 L^2 \alpha g \beta}{\rho_0 c_p} \right]^{1/3}, \quad T_0 = \left[\frac{L}{g\beta} \left(\frac{\alpha J_0}{\rho_0 c_p} \right)^2 \right]^{1/3}. \quad (39)$$

With this substitution of variables the system (2), (4) takes the following form:

$$\frac{\partial v}{\partial x} + \frac{1}{\rho} \frac{\partial}{\partial \rho} (\rho u) = 0,$$

$$v \frac{\partial \theta}{\partial x} + u \frac{\partial \theta}{\partial \rho} - \exp(-\alpha L x) I(x, \rho) = \left(\Delta_\perp \theta + \frac{1}{\gamma^2} \frac{\partial^2 \theta}{\partial x^2} \right) \Big/ \mathrm{Pr}\, Q^{1/3},$$

$$v \frac{\partial v}{\partial x} + u \frac{\partial v}{\partial \rho} + m\theta = -\frac{1}{\gamma^2} \frac{\partial}{\partial x} \left\{ \int_\rho^\infty d\rho' \left(v \frac{\partial u}{\partial x} + u \frac{\partial u}{\partial \rho'} \right) \right\} + \frac{\Delta_\perp^{-1}}{Q^{1/3}} \left(\Delta_\perp + \frac{1}{\gamma^2} \frac{\partial^2}{\partial x^2} \right)^2 v, \quad (40)$$

where Q is determined by expression (11). It follows from (40) that it is possible to ignore the action of thermal conductivity and viscosity in the vicinity of the heating beam if

$$Q^{1/3} \gg 1. \quad (41)$$

Relation (41) is the condition for well developed PC to occur in the fluid.

We also go over to dimensionless form in Eqs. (1). Using (5) (6), (39) and $s = qL/r_0$ we have

$$\frac{\partial I}{\partial x} + \frac{1}{\rho} \frac{\partial}{\partial \rho} (\rho s I) = 0, \quad \frac{\partial s}{\partial x} + s \frac{\partial s}{\partial \rho} = -D(L) \frac{\partial \theta}{\partial \rho}, \quad (42)$$

where

$$D(L) = \left[\left(\frac{1}{n_0} \left| \frac{dn}{dT} \right| \right)^3 \frac{L^7}{g\beta} \left(\frac{\alpha J_0}{\rho_0 c_p} \right)^2 \right]^{1/8}. \quad (43)$$

Expressions (39) are the characteristic velocity and temperature dependences of convective flow in well developed PC for $L \ll L_{\mathrm{NL}}$. From (42), (43) we have for the beam divergence in this case

$$\psi \sim \frac{1}{n_0} \left| \frac{dn}{dT} \right| \left[\frac{L^4}{g\beta r_0^3} \left(\frac{\alpha J_0}{\rho_0 c_p r_0^3} \right)^2 \right]^{1/8}.$$

Let relations (41) be valid and then, taking into account that $\gamma \gg 1$, the right-hand sides of the last two equations in the system (40) can be assumed to vanish. It is evident that the simplified system of hydrodynamic equations and Eqs. (42) so obtained can be characterized by a uniform random scale independent of the direction of light beam propagation.[1)] Therefore the characteristic thermal self-action length is determined from the relation $D(L_{\mathrm{NL}}) = 1$ in the following manner:

$$L_{\mathrm{NL}} = \left[\left(\frac{1}{n_0} \left| \frac{dn}{dT} \right| \right)^{-3} g\beta \left(\frac{\rho_0 c_p r_0^3}{\alpha J_0} \right)^2 \right]^{1/7}. \quad (44)$$

Estimates for the velocity and temperature scales of convective flow in the case $L_{\mathrm{NL}} \ll L$ are found from relations (39) in this case by replacing L with L_{NL} (44):

$$V \sim \left[\left(\frac{1}{n_0} \left| \frac{dn}{dT} \right| \right)^{-2} \frac{(g\beta)^3 \alpha J_0 r_0^4}{\rho_0 c_p} \right]^{1/7},$$

$$T \sim \left[\left(\frac{1}{n_0} \left| \frac{dn}{dT} \right| \right)^{-1} \left(\frac{r_0}{g\beta} \right)^2 \left(\frac{\alpha J_0}{\rho_0 c_p} \right)^4 \right]^{1/7},$$

while for the beam divergence we have

$$\psi \sim \frac{r_0}{L_{\mathrm{NL}}} \approx \left[\left(\frac{1}{n_0} \left| \frac{dn}{dT} \right| \right)^3 \frac{r_0}{g\beta} \left(\frac{\alpha J_0}{\rho_0 c_p} \right)^2 \right]^{1/7}.$$

In the discussions above the flow was assumed to be laminar and effects like the transaction to turbulence of the hydrodynamic flow were ignored. The generation thresholds of light-induced turbulence and its excitation by a vertical radiation beam has been examined in detail in Ref. 12.

5. EXPERIMENTAL RESULTS

A configuration in which the laser beam propagated upward was selected for the experiment. PES-4, PMS-20 and PMS-1000 organosilicon fluids were used as the irradiated media, which made it possible to vary the viscosity, coefficient of absorption and other parameters of the medium over a broad range. The fluid properties are given in the table. A $50 \times 60 \times 300$ mm silica glass cuvette was used whose bottom was placed 50 cm from the laser. The fluid layer height was 30, 90, and 180 mm. Nonlinear thermal effects of a CW YAG solid-state laser ($\lambda = 1.06$ μm) were investigated. Beam power was controlled over a range 14–74 W, with the measured beam radius at the fluid entrance varied from 2.4 to 4.4 mm. A more detailed description and a complete set of experimental data can be found in Ref. 13. Here we will only

TABLE I. Properties of organosilicon fluids.

	PES-4	PMS-20	PMS-1000
ρ, kg·m^{-3}	1100	940	980
ν, m^2·s^{-1}	$4.5\cdot10^{-5}$	$2\cdot10^{-5}$	10^{-3}
α, m^{-1}	5.94	1.83	1.84
c_p, J·kg^{-1}·K^{-1}	1863	1717	1633
β, K^{-1}	$7.3\cdot10^{-4}$	$9.7\cdot10^{-4}$	$8.7\cdot10^{-4}$
χ, m^2·s^{-1}	$7.2\cdot10^{-8}$	$8.5\cdot10^{-8}$	$9.8\cdot10^{-8}$
Pr	625	235	10 200

discuss the aspects directly related to the preceding discussion.

The values of the thermal complex Q' estimated on the basis of beam radius and power measurements for these experiments lay in the range 10^{-7}–10^{-1} and in this case the condition $10^{-4} \lesssim (\mathrm{Pr}^2 Q')^{-1} \lesssim 0.1$ held. The values of the right member of the inequality (38) varied from 0.2 and 0.8 in the experiment. Relations (38) therefore were satisfied and, consequently, it is possible to conclude that moderate convection was achieved in the experiment (a regime that has only been investigated numerically[4] to date). The theoretical results from Sec. 3 were therefore used to process the experimental data.

Before discussing experimental results we wish to draw attention to the following fact: A weak convection layer exists near the illuminated base. Based on the results from Ref. 11 it is possible to determine that in the range of fluid and beam parameters implemented in the experiment the existence of even a very thin (compared to the total fluid height) layer $\sim r_0$ with such a condition can produce significant beam divergence. It is therefore necessary to estimate the possible influence of this layer on experimental results. This can be done in the following manner. We decompose the layer on the longitudinal coordinate into two halves and assume in the first half ($z > z'$) that the axial flow velocity is described by expression (20), and that it is necessary to take into account the condition $V|_{z=0} = 0$ in the second half near the upper boundary. In dimensionless variables the equation for the axial flow velocity in the second region takes the form

$$\frac{2}{\gamma^2}\frac{\partial^2}{\partial x^2} v(x,0) = \theta(x,0).$$

Taking into account the natural free-surface boundary condition $\partial\theta/\partial x = 0$, we can set $\theta(x) \approx \theta(x') \approx \theta(0)$ in this equation. It is then easy to obtain an expression for $v(x,0)$ for $x < x'$ proceeding from the velocity mixing condition at the boundary of the two regions $x = x'$. An estimate of the thickness of layer z'' with weak convection is then found from the relation $v(x'',0) \sim \mathrm{Pr}^{-1} Q^{-1/2}$ in the following form:

$$z'' \sim r_0 \left(\frac{L}{L_{\mathrm{NL}}}\right)^{1/2} \Big/ \mathrm{Pr}\, Q^{1/2}.$$

For the experiment described here we have $z'' \ll r_0$ and the possible contribution of the immobile medium layer of this thickness to the beam divergence is two orders of magnitude less than that observed. It is therefore quite valid to ignore this layer both in the theoretical analysis and in the examination of the experiment data.

The angular divergences (across the slot in the focal plane of the lens) were measured in the experiment by means of an IR visualizer together with the laser beam radii ahead of (r_0) and beyond (r) the fluid layer. Figure 1 gives the results from such an investigation of thermal self-action. Figure 1(a) provides the experimental dependences of the angular divergences ψ of the laser beams on power P for various fluid column heights and types. The power dependence of the beam radius at the fluid exit has an analogous form. The theoretical analysis provided here makes it possible to fit the results of the entire series of measurements with a single description. An expression was derived in Sec. 3 for a parameter L_{NL} that determines nonlinear laser beam effects. The results from this qualitative analysis can be formulated in the following manner: For $H/L_{\mathrm{NL}} < 1$ the dimensionless divergences $\psi H/r_0$ and the radii r/r_0 of the beams will be linear functions of the dimensionless distance H/L_{NL}. Figures 1(b) and (c) give the test results of these regularities where L_{NL} were calculated for formula (30). The straight lines in the curves, generated by the method of least squares, clearly reveal the agreement between experimental results and theoretical conclusions.

The velocities and temperatures of photoabsorption convection flows were also measured in the experiment. The velocities were measured by a DISA laser Doppler anemometer. A remote optical method of sensing variations in the

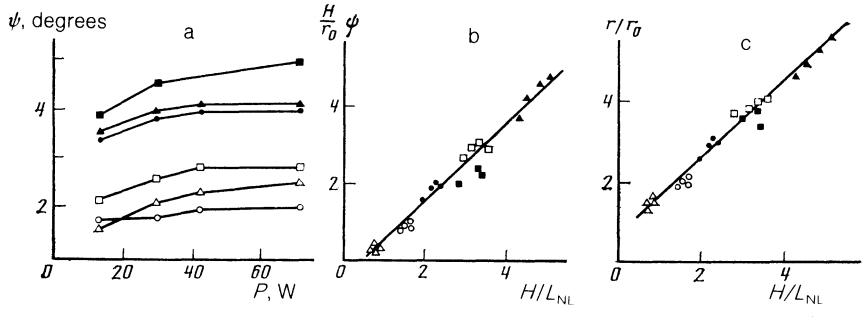

FIG. 1. Experimental plots of the divergence ψ of the laser beams as a function of power (a), the "dimensionless" divergence $\psi H/r_0$ as a function of the parameter H/L_{NL} (b) and the dimensionless radius r/r_0 as a function of the parameter H/L_{NL} (c): ○—PMS-20, $H = 90$ mm; ●—PES-4, $H = 30$ mm; △—PMS-20, $H = 180$ mm; ▲—PES-4, $H = 90$ mm; □—PES-4, $H = 180$ mm; ■—PMS-1000, $H = 90$ mm.

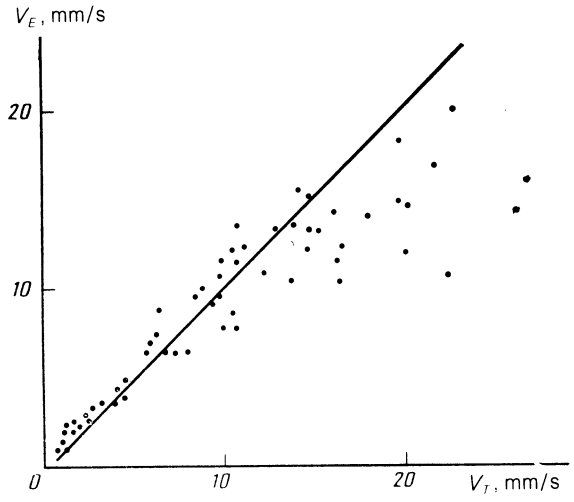

FIG. 2. Comparison of the experimental V_E and the theoretical V_T [calculated by (14)] values of the axial convective flow velocity. The straight line corresponds to $V_E = V_T$.

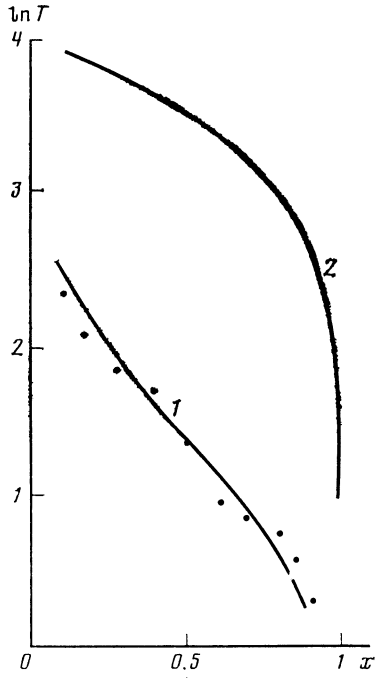

FIG. 4. Horizontal temperature distribution along the convective flow axis for PES-4 fluid for $P = 45$ W, $H = 180$ mm. The circles represent the experimental values; curve 1 represents calculation by formula (34) for $C = 0.2$, curve 2 represents calculation by (34) for a prescribed beam; $R(\xi) = 1$, i.e., ignoring nonlinear effects.

refractive index of a medium that in this case are unambiguously related to the spatial temperature distribution was used to obtain the induced temperature profiles. A narrow helium-neon laser probe beam was used; this beam was refracted by the temperature irregularities as it propagated through the fluid. The refraction angle of the horizontal beam was measured in the experiment as a function of the impact parameter, which is sufficient for recovery of the perturbation potential in the case of cylindrical symmetry.[14]

Figures 2 and 3 give the results from a comparison of the measured axial flow velocities and the theoretical values calculated by Eq. (20), where the function $r(\xi)$ was estimated from the beam divergence by a linear law and Λ was taken as 27 mm. Figure 3 reflects the ratio of experimental and theoretical values as a function of the dimensionless cross-section coordinates in which the measurements were carried out. The solid circles represent the average values of the V_E/V_T ratio, while the vertical lines reflect a 95% confidence range. Averaging was carried out over the values of this ratio obtained across the entire range of parameters that were varied in the course of the experiment. Sampling size was > 10 for each point. The deviation of the V_E/V_T ratio from unity for $x = 0.16$ can be attributed to the influence of the free surface ($x = 0$) on the experimentally measured velocity, which was not taken into account in Eq. (20). The deviation of the experimental points from the $V_E = V_T$ line in Fig. 2 with large values of V_T that correspond specifically to $x = 0.16$ has an analogous explanation.

A direct comparison of the measured temperatures to expression (34) was impossible, since the axial beam intensity at the fluid boundary, which was not measured, enters into the calculation formula through the constant C. However expression (34) can be considered as a relation for determining the constant C based on experimental data if the measured temperature values are substituted into its left side. It follows from the entire set of values obtained in this manner that $C = 0.2 \pm 0.03$. Figure 4 gives the experimental points and theoretically calculated horizontal temperature distribution for $C = 0.2$ (curve 1) along the flow axis in PES-4 fluid for $P = 45$ W, $H = 180$ mm as an example demonstrating good agreement beween experiment and theory. Figure 4 also provides the temperature distribution in the fluid that would exist in the absence of beam nonlinear effects (curve 2) for comparison purposes.

In conclusion the authors wish to express their gratitude to V. I. Tatarskii, A. S. Gurvich, V. V. Vorobev and B. S. Agrovskii for their extensive commentary, advice and assistance in this study.

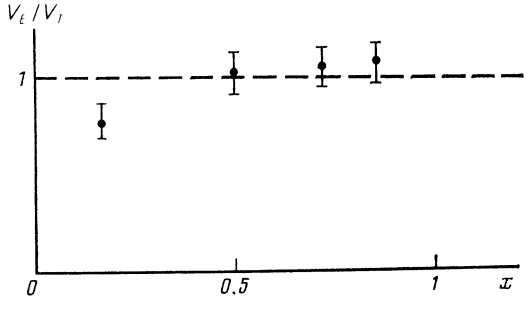

FIG. 3. V_E/V_T ratio plotted as a function of the dimensionless coordinate $x = z/H$ of the cross section. The solid circles represent the sample mean, and the vertical lines represent the confidence range at 0.95.

[1)]We note that this is not the case for moderate PC. The characteristic longitudinal scale for velocity is the length over which energy is absorbed from the beam, while the characteristic scale for temperature is min L, $\{L_{NL}\}$.

[1]D. K. Smith, Proc. IEEE. **65**, 59 (1977).
[2]V. A. Petrishchev, L. V. Piskunova, V. I. Talanov and R. M. Erm, Izv. Vyssh. Uchebn. zaved. Radiofiz. **24**, 161 (1981).
[3]V. V. Vorob'ev and V. V. Shemetov, Izv. Vyssh. Uchebn. zaved. Radiofiz. **22**, 441 (1979).
[4]B. P. Gerasimov, V. M. Gordienko, I. S. Kalachinskaya and A. P. Sukhorukov, Preprint of the Institute of Applied Mathematics of the USSR Academy of Sciences No. 63 (1975).
[5]W. G. Wagner and J. H. MacBurger, Opt. Comm. **3**, 19 (1971).
[6]B. P. Gerasimov, V. M. Gordienko, and A. P. Sukhorukov, Zh. Tekh. Fiz. **45**, 2485 (1975) [Sov. Phys.—Tech. Phys. **20**, 1551 (1975)].
[7]B. P. Gerasimov, V. M. Gordienko, and A. P. Sukhorukov, Inzh.-fiz. zhurn. **33**, 705 (1977).
[8]B. P. Gerasimov, V. M. Gordienko, and A. P. Sukorukov, Inzh.-fiz. zhurn. **36**, 331 (1979).
[9]L. D. Landau and E. M. Lifshits, *Fluid Dynamics, 2nd ed.*, Pergamon, Oxford (1987), ch. 2.
[10]N. E. Galich, O. G. Martynenko, V. Yu. Pochekutov, and Zh. Z. Ustok, Kvant. Elekt. **11**, 148 (1984) [Sov. J. Quantum Electron. **11**, 81 (1981)].
[11]V. A. Aleshkevich, A. V. Migulin, A. P. Sukhorukov, and E. N. Shumilov, Zh. Eksp. Theor. Fiz. **62**, 551 (1972) [Sov. Phys. JETP **35**, 292 (1972)].
[12]N. E. Galich, Zh. Tekh. Fiz. **55**, 1473 (1985) [Sov. Phys.—Tech. Phys. **30**, 853 (1985)].
[13]A. S. Gurvich and V. I. Zuev, Preprint of the Institute of Atmospheric Physics of the Academy of Sciences of the USSR. (1987).
[14]S. V. Sokolovskii, Izv. AN SSSR. Fizika atmosfery i okeana. **17**, 574 (1981).

Translated by Kevin S. Hendzel